Mitigation Solutions for the Magnetic Field Produced by MFDC Spot Welding Guns

Mitigation solutions for the magnetic field produced by MFDC spot welding guns

Luca Giaccone, *Senior, IEEE*, Vincenzo Cirimele, *Member, IEEE,* and Aldo Canova, *Senior, IEEE*

***Abstract*—Among the different welding technologies, portable welding guns are one of the most critical devices in relation to human exposure to electromagnetic fields. This paper focuses on medium frequency direct current guns proposing two actions aimed to the mitigation of the magnetic field generated during the welding process. The first action consists in the adoption of a passive shield for the on-board medium frequency transformer. The analysis points out that the transformer alone produces a magnetic field that can exceed the prescribed limits. Therefore, a suitable mitigation system is identified. The second action aims to mitigate the predominant magnetic field that is generated by the electrodes of the welding gun. The analysis of the field waveforms shows that the rise time of the welding current pulse is the main parameter affecting the exposure index. The effect of the increase of the rise time is investigated through experimental and numerical analyses. The results prove that a small increase of the rise time causes a significant reduction of the exposure level. It is noteworthy that the two mitigation actions can be adopted on both existing and newly developed welding guns as they do not require any structural modification of the welding device.**

***Index Terms*—Welding, magnetic shielding, magnetic fields, dosimetry, numerical analysis.**

I. Introduction

RESISTANCE spot welding (RSW) is a commonly employed technology in the industry sector. RSW devices are mainly subdivided in two categories: *medium frequency direct current* (MFDC) and *alternating current* (AC). MFDC guns are often preferred to the AC ones thanks to some benefits. The MFDC guns require a shorter weld time resulting in a significant energy saving. Moreover, MFDC systems are very stable in working conditions far from the rating power (useful range: 20-95%). Conversely, AC systems are unstable and inefficient when used outside the 70-90% of the rating power.

In the automotive sector, a huge percentage of the assembly procedure relies on RSW. That is why RSW has been widely investigated focusing the attention on different topics. In the current literature, several papers that develop suitable methods for improving the quality of the welding process can be found [1]–[5]. In this paper the attention is focused on an unwanted effect of the MFDC welding systems: the generation of very high values of magnetic field in the region nearby the device. Standards and guidelines related to the human exposure to electromagnetic fields are mainly provided by the Institute of Electrical and Electronic Engineers (IEEE) [6], [7] and the International Commission on Non Ionizing Radiation Protection (ICNIRP) [8]–[10]. In both cases it is identified an exposure quantity directly related to adverse biological effects. The exposure quantities have to be limited below the prescribed values that are called *basic restrictions*. By means of dosimetric models, it is possible to compute the maximum permissible values of the external field (electric or magnetic field) able to induce such basic restrictions. These maximum permissible values are also called *reference levels* and they are often computed using simple and conservative dosimetric models. Furthermore, since other additional safety factors are introduced, it is possible to say that, if external field values are below the reference levels, the exposure quantities are well below the basic restrictions. Conversely, the exceeding of the reference levels does not necessarily imply the exceeding of the basic restrictions. Bearing all this in mind, for simple sources of electric or magnetic fields, the literature provides several mitigation solutions aimed to reduce the external field below the reference levels [11]–[17]. However, there are other field sources for which the design or the installation of a mitigation system is not sufficient or not possible at all. RSW devices, induction heating systems and also new emerging technologies based on the inductive power transfer are possible examples. In these cases the human exposure is assessed by means of a dosimetric analysis and usually, since the exposure is highly non-uniform, basic restrictions are satisfied even if reference level are largely exceeded [18]–[23].

Among all general aspects, a subject with particular importance is the protection of the working population against the possible effects caused by electromagnetic fields. This is also a concern of the European Community that provided several directives. The first European Directive in which the problem was addressed [24] has been repealed and substituted by a newer reference in 2013 [25]. Both directives refer to the ICNIRP guidelines and the rationale behind the protection is not modified by the new directive. Only short-term effects are taken into account because the current scientific community does not take a common position regarding the possible long-term effects caused by electromagnetic fields. The latest European Directive refers to the newest ICNIRP guidelines [10]. As a consequence, reference levels and basic restrictions are changed with respect to the older ones [8]. Finally, more detailed information is given for the analysis of complex and pulsed waveforms. In this paper, unless otherwise stated, the 2010 ICNIRP limits for occupational exposure will be used as a reference.

The shielding of the welder terminals represents a technical challenge due to the operating use of this system that makes practically impossible the application of an adequate shielding system able to work in all the working conditions. Nevertheless, it is important to try to protect the welding operators as much as possible. This is the starting point of the present paper that focuses on two actions aimed to mitigate the magnetic field produced by MFDC guns. These actions aim to decrease

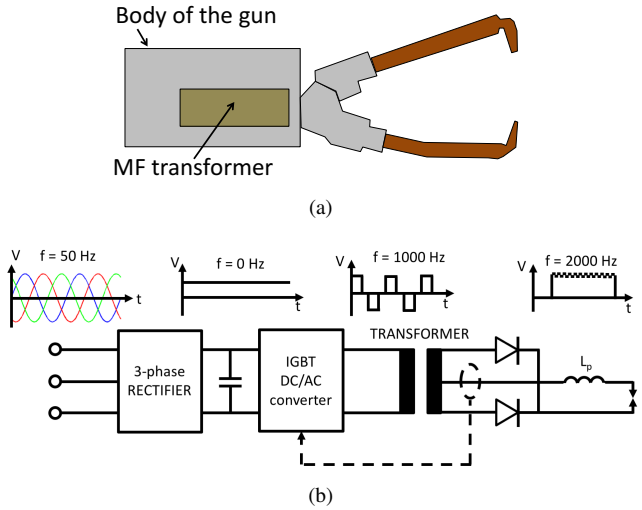

Fig. 1. Layout of an MFDC welding gun (a) and scheme of the supply chain of the MFDC welding system (b). The welding gun is supplied from the standard 3-phase-50 Hz distribution. The AC signal is then rectified and filtered obtaining a DC signal at the DC/AC converter input. The DC/AC converter provides a square wave AC signal at 1000 Hz used to supply the on board transformer. At the transformer output, the AC signal is rectified by means of a full-wave diode rectifier that provides the welding DC signal. The absence of filters leaves a superposed ripple at two times the frequency of the rectified signal (2000 Hz).

the exposure levels improving the protection of the operators that have to work in close proximity to the welding gun body. The first action is focused on an essential device installed on the welding gun framework that is the medium frequency (MF) transformer. It is found that the transformer alone can generate a magnetic field that exceeds the reference levels provided by the ICNIRP for occupational exposure. For this reason, we propose a mitigation system to bring emissions under the allowed values. In order to point out what is the best solution for this kind of magnetic field source several shielding configurations are tested. The second action focuses on the modification of the welding current pulse parameters as a way to modify its spectrum in the range that causes the maximum exposure.

II. Description of the Magnetic Field Source

A. MFDC welding system

A typical MFDC welding gun is represented in Fig. 1(a). Welding processes require high current values that are obtained by means of the MF on board transformer (also represented in Fig. 1(a)). The whole supply chain of these devices is shown in Fig. 1(b). It is composed by an IGBT H-bridge and a center tapped transformer. The latter is used together with a full-wave diode rectifier directly linked to the welder terminals and integrated in the transformer framework.

The voltage supplied by the H-bridge is a square wave at 1000 Hz that, at the rectifier output, results in a DC current. The conversion process generates a 2000 Hz ripple and higher harmonics superposed on the DC level. The IGBT converter can provide different partializations of the voltage waveform to regulate the value of the welding current. The welding

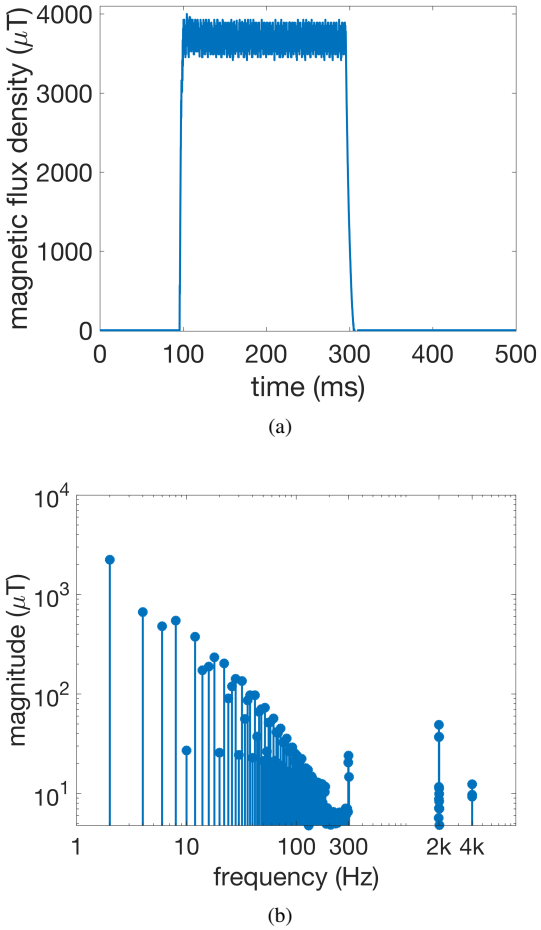

Fig. 2. Example of magnetic field waveform registered close to an MFDC gun (a). Spectrum of the magnetic field: most of the spectral lines are concentrated below 300 Hz and other not negligible components can be observed at 2 kHz and 4 kHz (b).

process can be performed by one or more pulses. Each pulse is completely described by the following parameters:

1) *current peak*: the maximum value that the current reaches during the pulse;
2) *weld time*: the duration of the pulse;
3) *rise and fall time*: time needed to bring the current from zero to the peak and vice versa.

The rated current can reach very high values (20/30 kA) however, for common welding processes, the current is set in the range $[5, 10]$ kA. The rise time can be regulated by setting the DC/AC converter, and the current peak is reached via a ramp variation.

Since the magnetic field is proportional to the current, it will be pulsed as well and with a relevant harmonic content. An example of magnetic flux density waveform registered close to an MFDC gun is shown in Fig. 2(a). Only one component of the field is shown without loss of generality. The spectrum of this waveform is shown in Fig. 2(b). Most of the spectral lines are concentrated below 300 Hz and other not negligible components can be observed at 2 kHz and 4 kHz. Also frequency components higher than 4 kHz can be observed when the welding current is lower than the rated one.

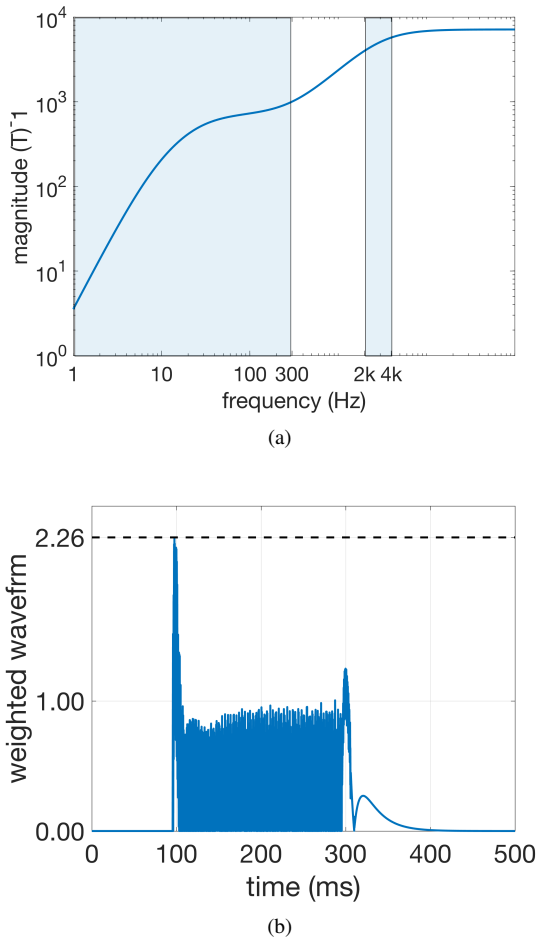

Fig. 3. Example of MFDC pulsed field (a). Example of processing by means of WPM (reference levels for occupational exposure proposed by the ICNIRP are considered [10]) (b).

B. Pulsed magnetic fields assessment

Pulsed magnetic fields have to be assessed with suitable methods. The ICNIRP, the IEEE and also other scientists suggested more than one suitable methodology [6], [7], [9], [26], [27]. In this paper we refer to the well known approach called weighted peak method (WPM). In short, according to the WPM, the exposure is considered compliant if the following expression is satisfied at any time:

$$I_{\mathrm{WP}} = \left| \sum_{\mathrm{j}} \frac{A_{\mathrm{j}}}{A_{\mathrm{lim,j}}} \cos\left(2\pi f_{\mathrm{j}} t + \theta_{\mathrm{j}} + \varphi_{\mathrm{j}}\right) \right| < 1 \qquad (1)$$

being A_{j} the quantity to be assessed at frequency j, $A_{\mathrm{lim,j}}$ the limit for this quantity at frequency j. θ_{j} is the phase of A_{j} and φ_{j} is the phase of $A_{\mathrm{lim,j}}$.

The WPM can be interpreted as a high-pass filter whose frequency response has magnitude equal to $1/A_{\mathrm{lim,j}}$ and the phase is φ_{j} [9], [10], [28]. Considering the 2010 ICNIRP limit for occupational exposure, the magnitude of this filter is represented in Fig. 3(a) [10]. Two transparent boxes also highlight the frequency ranges where the spectrum of the magnetic field in Fig. 2(a) is concentrated.

The application of the WPM to the waveform in Fig. 2(a) provides the weighted waveform in Fig. 3(b). This waveform corresponds to the left hand side of eq. (1) and, in the present example, the magnetic flux density does not satisfy eq. (1) because the peak is > 1. It is worth nothing that the peak of the weighted waveform is registered during the slope-up of the magnetic field. This concept will be exploited later, in section IV.

C. Mitigation actions

Several practical measurement campaigns and exposure assessment activities conducted on MFDC welding guns enabled us to find out two particular actions aimed to strongly mitigate the exposure levels to them related.

The first action investigates the effectiveness of passive shields made of metallic enclosures. Of course they cannot be applied to the gun arms because they would make impractical or impossible the welding process. These passive shields are tested for the mitigation of the magnetic field generated by the MF transformer. Even if several works about MFDC guns [19], [20], [29]–[33] and also the main standards related to welding process [34], [35] consider the contribution of the MF transformer as negligible, by means of measurements, we registered magnetic field values higher than reference levels considering the transformer alone (not embedded in the gun). Considering that the pelvic area of the operator is quite close to the transformer during the welding and seeking the principle of due diligence aiming to reduce as much as possible the exposure, we propose a method to reduce the contribution to the emission given by the MF transformer which is not covered by the current literature.

The second action focuses on the most significant exposure aspect: the magnetic field created by the gun arms. As it is shown in Fig. 3(b), the maximum exposure is registered during the slope-up. This suggests that the rise time of the welding current (equal to rise time of the magnetic field waveform) could modify the exposure conditions. Therefore, we investigated the influence of this parameter on the exposure obtaining relevant results.

As a final remark, it is important to say that the application of both actions did not require any modifications in the welding gun architecture. Passive shields can be installed in the already existing mechanical structure of the gun and the rise time of the welding current can be tuned by means of the standard control system. Hence, both actions can be generally and immediately applied to every MFDC welding gun (also the existing ones). In the following, each mitigation action is analyzed separately.

III. MF Transformer Mitigation Solutions

The current literature on shielding systems provides several solutions suitable for a huge number of mitigation problems [11]–[17]. Low frequency magnetic fields are usually mitigated by means of metallic plates. The shield is selected according to the mitigation requirements and it is common to select among materials with high conductivity or materials with high permeability. Sometimes the combination of both materials is required to reach the desired mitigation [36]. For simple sources,

it is generally well known how to select a proper configuration and a suitable material. In the case under analysis, the MF transformer generates a pulsed magnetic field that makes it difficult to predict which material and configuration provide the best results. Hence, five configurations were selected and tested to make a comparative analysis:

1) **Pure iron**: 2 plates with thickness 0.5 mm (2×0.5 mm).
2) **Grain oriented** steel sheet with **single orientation**: 2 plates with thickness 0.35 mm (FeGO single 2×0.35 mm).
3) **Grain oriented** steel sheet with **double orientation**: 2 plates with thickness 0.35 mm (FeGO double 2×0.35 mm).
4) **MuMETAL**[1]: 1 layer with thickness 0.127 mm (Mu 1×0.127 mm).
5) **Aluminum**: 1 layer with thickness 1 mm (Al 1×1 mm).

Each configuration encloses the transformer as shown in Fig. 4. Moreover, all the solutions are proposed according to the limitation in space and weight imposed by the application and the mechanical allocation of the transformer in the welding system. These constraints pose a limit to the thickness of the materials and on the dimension of the enclosure.

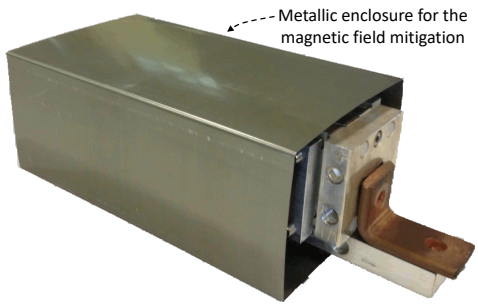

Fig. 4. Shape of the shielding magnetic enclosure.

Regarding the proposed mitigation solutions, it is necessary to provide some additional details regarding the ones that make use of FeGO. As indicated in the configuration list, solution 2 uses a single orientation of the grains whereas solution 3 has a double orientation. To better understand these configurations it is possible to look at Fig. 5 where the orientation is represented graphically. We decided to investigate both configurations because it is not known a priori where the leakage flux is prevalent.

A. Test conditions

The tests are performed using a supply system that generates a square waveform of ± 130 V at 1000 Hz reproducing, at the rectifier output, a welding pulse having the following parameters:

- rise time: 1 ms (one cycle of the 1000 Hz supply waveform);
- current peak: 5 kA;
- weld time: 100 ms;
- fall time: 1 ms (one cycle of the 1000 Hz supply waveform).

[1]MuMETAL is an alloy with very high initial permeability. A common composition is: Ni 81%, Mo 5%, Si 0.4%, Mn 0.5%, C 0.01%, Fe 13.09%.

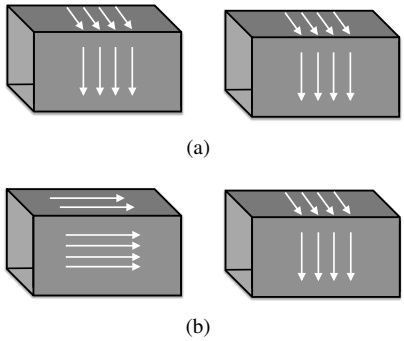

Fig. 5. Representation of the two different solution with sheets with the same grane orientation (a) and with different grane orientation (b).

The measured waveforms related to the welding pulse are shown in Fig. 6. The current waveform represented in Fig. 6 reaches a peak and then decreases during the pulse. This decrease is not physical and it is related to the adopted current probe bandwidth. In particular, in our case, the physical dimension of the transformer and the available space allowed exclusively the use of a flexible Rogowski coil. This kind of probe is able to measure currents with a lowest frequency of 1 Hz. The impossibility to measure the DC component of the current is the cause of the constant decrease during time. This effect is detailed in [37].

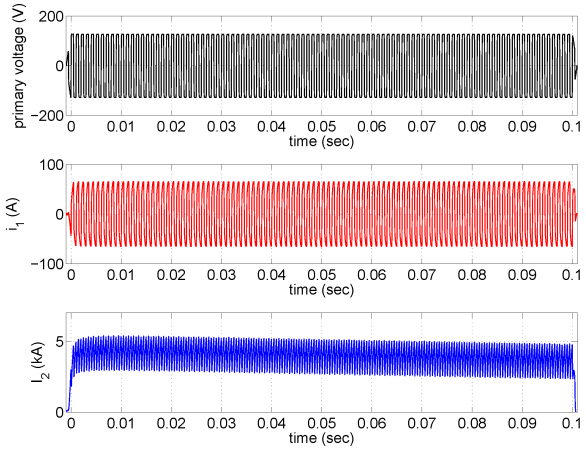

Fig. 6. Waveforms of the welding pulse. Voltage at the primary side of the transformer input in gray, primary current in red, rectified current at the welder terminals in blue.

Finally, an auxiliary coil wounded around one wall of each shield. This coil was used to measure the induced voltage during the tests to obtain the magnetic flux density inside the material by integrating over time. With this auxiliary coil we verified that all the proposed shields were far from the saturation.

B. Reference system and measurement points

The comparison among the investigated mitigation solutions is based on the measurements provided in repetitive inspection

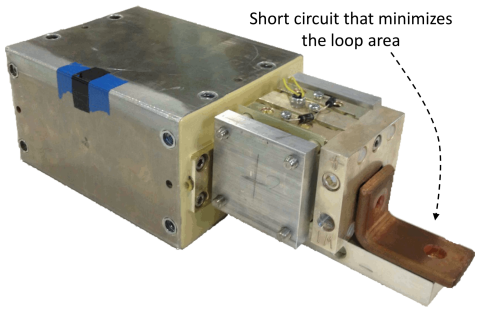

Fig. 7. Description of the short circuit connection that minimize the effect of the transformer secondary.

points. To have significant measurements, the inspection points are selected so that the maximum distance is no higher than the maximum dimension of the transformer shown in Fig. 8. Taking as reference the surface of the metallic enclosure of the transformer, four inspection points $\mathrm{P}_1, \mathrm{P}_2, \mathrm{P}_3, \mathrm{P}_4$ at two different distances of 10 and 20 cm are defined according to the representation of Fig. 9. The blue reference system identifies the measured components of the magnetic field. The maximum distance of 20 cm from the surface of the transformer is decided considering that the magnetic field decreases quickly moving away from the transformer.

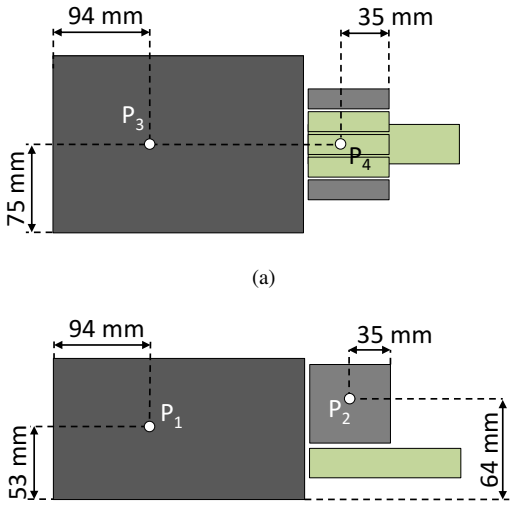

Fig. 8. Representation of the transformer in the XY plane (a) and in the XZ plane (b) with main dimensions.

The measurements of the three orthogonal components of the magnetic field are carried out by means of an isotropic probe as suggested by ICNIRP guidelines and standards [10], [34]. The magnetic field meter used is the NARDA ELT-400 whose bandwidth is 1 $\mathrm{Hz} - 400$ kHz. This instrument is endowed by two probes with different coil dimension of 3 cm^2 and 100 cm^2. The measurements presented in this paper have been carried out using the smaller probe.

Among all measured waveforms, Fig. 10 shows 15 ms of the three components measured at P_1 (distance 10 cm) without

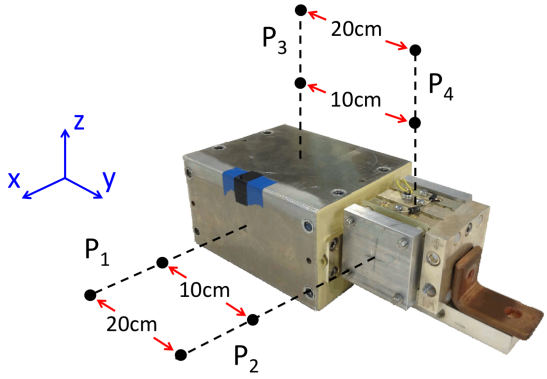

Fig. 9. Reference system and measurement points for the magnetic field evaluation.

the shield (i.e. only source) and with two shielding solutions: pure iron and aluminum.

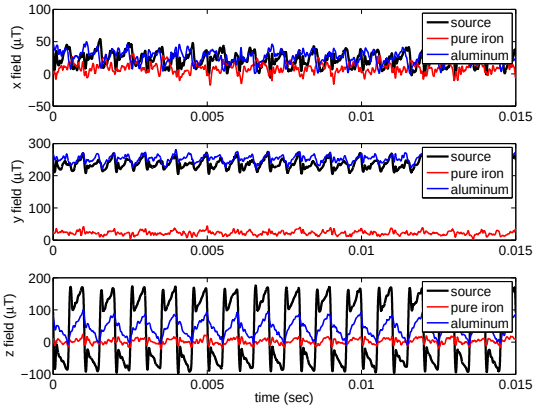

Fig. 10. Waveforms of the measured components of the axis x,y,z of the magnetic flux density of the only MF transformer and the same components in presence of aluminum or pure iron shield.

C. Characterization of the shielding solutions in terms of exposure

Passive shield performance is usually quantified with the shielding factor (SF). The SF is a pointwise function of the space and it is defined as the ratio between the unmitigated and the mitigated field at a given point [14]. In the application under analysis, the magnetic field waveform is pulsed and, therefore, the SF should be computed for the whole spectrum giving rise to many results that can be hardly interpreted to find the best shielding configuration. Therefore, we propose to use the WPM to select the shield. In fact, the WPM analyzes the field waveforms providing a single scalar value that is representative of the exposure taking into account all the spectrum at once.

Considering the reference levels provided by the ICNIRP 2010 guidelines, the magnetic field waveforms registered at all the inspection points have been processed with the WPM obtaining the results shown in Table I. From these results, is not possible to identify a solution that outperforms all

TABLE I
I_{WP} INDEX REFERRED TO THE 2010 VERSION OF THE ICNIRP GUIDELINES

	field point	source	pure iron	FeGO single	FeGO double	Mu	Al
10 cm	P_1	1.04	0.16	0.19	0.20	0.75	0.22
	P_2	1.44	0.27	0.42	0.40	1.07	0.51
	P_3	1.16	0.33	0.29	0.36	0.75	0.33
	P_4	1.55	0.45	0.49	0.54	1.28	0.50
20 cm	P_1	0.58	0.16	0.16	0.18	0.47	0.23
	P_2	0.62	0.17	0.15	0.19	0.51	0.21
	P_3	0.50	0.19	0.21	0.23	0.36	0.30
	P_4	0.53	0.25	0.27	0.29	0.56	0.34

the others for every field point. However, it is apparent that the shield made of pure iron is the solution to be preferred because it behaves better than the other shields in most of the measurement points.

At the same time, the results of Table I point out that the ICNIRP limits can be exceeded ($I_{\mathrm{WP}} > 1$) in the region close to the transformer. This confirms that the MF transformer can be an important source of magnetic field. Finally, it is shown that the index I_{WP} can be conveniently reduced by the use of a simple solution: a thin layer of pure iron around the transformer.

IV. VARIATION OF THE WELDING PULSE PARAMETERS

The conclusions drawn from the analysis of the I_{WP} and its correlation with the weighted waveforms give the base for the second strong and incisive mitigation action consisting in the regulation of the rise time of the welding pulse (hereinafter RT). The RT is the time interval between the beginning of the current ramp and the achievement of the set up current peak. This parameter is readily available in the control panel of RSW guns, therefore, it can be easily adjusted. Fig. 11(a) represents the same welding current with four different RT values. It must be stressed that $RT = 0$ ms is an abstraction because, even setting RT to zero, the current reaches the peak in $\approx$ 3 ms for physical reasons. Conversely, all the other values from 10 to 30 ms are the exact RT within the tolerance of the control system. The manufacturer guaranteed that all the analyzed RT values do not affect the quality of welding process.

As shown in Fig. 11(b), the increase of the RT reduces the spectral components roughly between 10 Hz and 200 Hz. Therefore, a mitigation effect is expected. This effect is studied in sections IV-A and IV-B by considering the magnetic flux density generated by the gun. Finally, the operator body is introduced in sections IV-C and IV-D. For a worst case scenario, magnetic flux density and induced electric field are computed and then processed with the WPM.

In all sections, when the magnetic field is computed, only the predominant field generated by the electrodes is considered.

A. Influence of the delay on reference levels

The magnetic flux density is measured at a fixed inspection point 0.5 m away from the gun laying on the axis of the loop

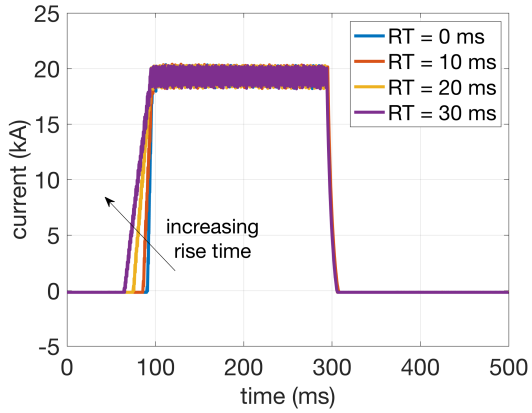

(a)

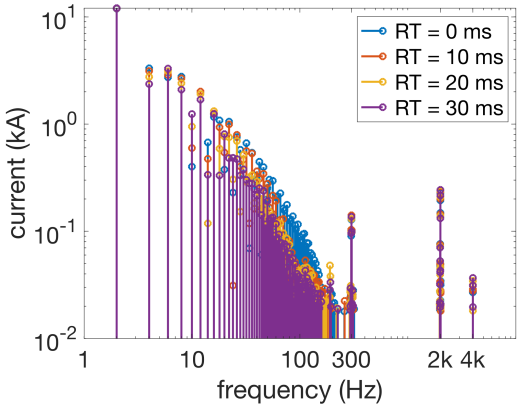

(b)

Fig. 11. (Waveforms of the four test currents with different delays: no delay, 10 ms delay, 20 ms delay, 30 ms delay (a). Relative spectrum (b).

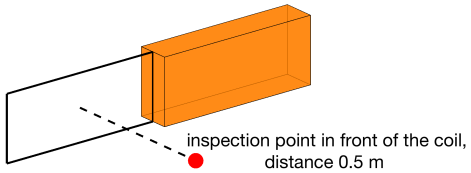

Fig. 12. Description of the inspection point for the measurements aimed to investigate the influence of the RT.

formed by the welding electrodes as shown in Fig. 12. The application of the WPM provides the weighted waveforms in Fig. 13 where the important role of the RT on the exposure becomes apparent. In fact, with respect to the reference case with $RT = 0$ ms, the peak of the weighted waveforms is strongly reduced and, in one case, this value is lower than 1 (i.e. compliant).

The same effect is evaluated for different values of the welding peak current. Fig. 14 summarizes these results by putting in correlation the maximum reached value of the weighted waveforms for different values of current peak and RT. It clearly appears that, for the cases at 10, 15 and 20 kA,

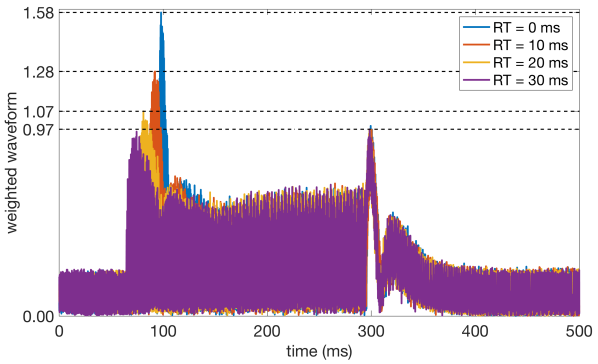

Fig. 13. Effect of the rise time on the weighted waveforms. It is shown the role of the rise time on the reduction of the peak (i.e. exposure index).

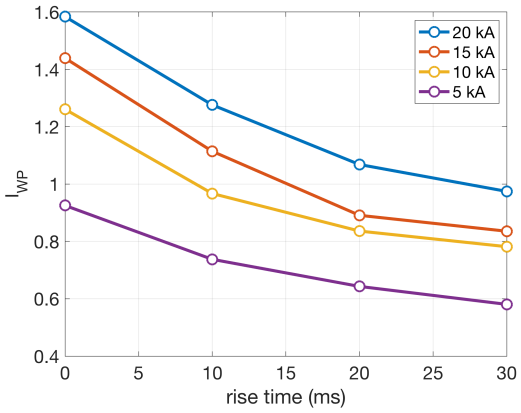

Fig. 14. Correlation between exposure index and rise time for different current peaks.

the increase of RT represents an effective mitigation solution that allows to comply with reference levels ($I_{WP} < 1$).

B. Safety distances

The effect of the RT is shown also computing the safety distance, i.e. the distance from the welding gun that guarantees the compliance with reference levels. For complex sources the safety distance is a 3D concept, it consists in the boundary of the volume outside which the compliance with reference levels is met. In this paper we represent this boundary with two cut planes of this volume. For the current of 20 kA, top and side view of the safety distance are shown in Fig. 15(a) and Fig. 15(b), respectively. It is apparent that the increase of the RT value makes it possible to decrease the safety distance from the gun. The extrema of the curves represented in Fig. 15 are reported in Table II.

Although the safety distance decreases by increasing the RT, reference levels are still exceeded in close proximity to the welding gun where the operator can stay during the welding operations. For this reason, a dosimetry assessment is performed in the next section.

C. B-field vs. Reference levels ($I_{\mathrm{p}} = 20$ kA)

The dosimetric assessment is made considering the worst case exposure scenario: the gun is in vertical position in front

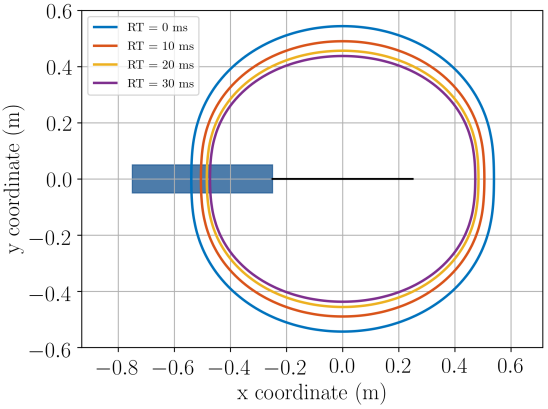

(a) Top view

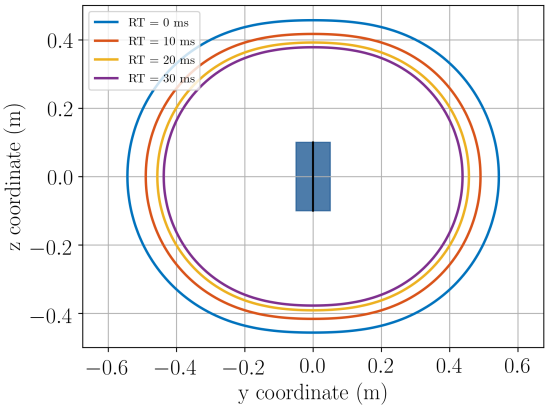

(b) Side view

Fig. 15. Safety area related to occupational exposure. Effects of the rise time for a fixed current of 20 kA.

TABLE II
EXTREMA OF THE SAFETY AREA, ICNIRP 2010 OCCUPATIONAL

current peak 20 kA	$x_{\min}$ (m)	$x_{\max}$ (m)	$y_{\min}$ (m)	$y_{\max}$ (m)	$z_{\min}$ (m)	$z_{\max}$ (m)
RT = 0 ms	-0.54	0.54	-0.54	0.54	-0.46	0.46
RT = 10 ms	-0.51	0.51	-0.49	0.49	-0.42	0.42
RT = 20 ms	-0.48	0.48	-0.46	0.46	-0.39	0.39
RT = 30 ms	-0.47	0.47	-0.44	0.44	-0.38	0.38

of the operator and the electrodes form a loop that lays in a plane parallel to the coronal plane [38]. It is quite easy to plot the exposure index related to the B-field over the human body because the magnetic field created by the induced currents is small with respect to the one created by the source currents [39]. Under this hypothesis, the magnetic field distribution is not perturbed by the eddy currents, so it can be computed independently of the conducting body. Therefore, the magnetic flux density is simulated in time domain and then processed with the WPM obtaining the exposure index at each voxel. The Duke model of the Virtual Family [40] is used to represent the gun operator and the configuration analyzed in this paper is shown in Fig. 16.

The values of the exposure index related to the magnetic

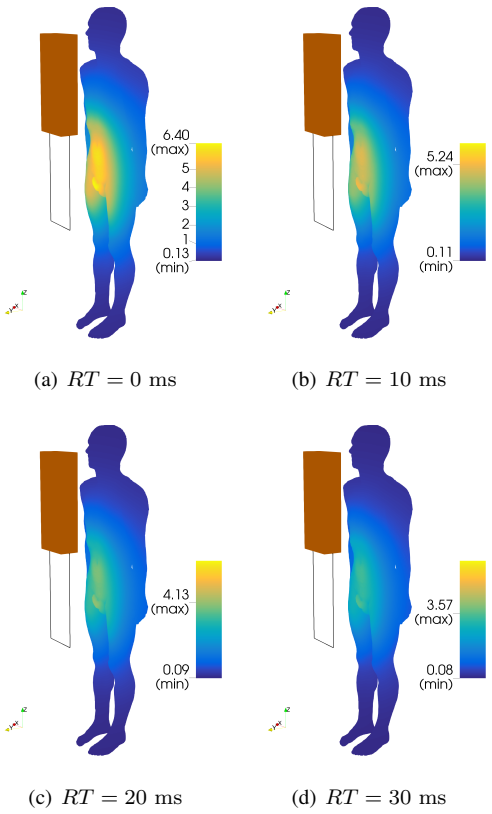

(a) $RT = 0$ ms (b) $RT = 10$ ms

(c) $RT = 20$ ms (d) $RT = 30$ ms

Fig. 16. Exposure index related to the magnetic flux density over the human body. The value of the exposure index reduces from 6.40 to 3.57 when passing from $RT = 0$ ms to $RT = 30$ ms, respectively.

flux density on the surface of the human body are represented through a color map. The exposure index is practically halved when passing from $RT = 0$ ms to $RT = 30$ ms.

D. Induced E-field vs. Basic restrictions ($I_{\mathrm{p}} = 20$ kA)

As claimed by the ICNIRP guidelines, since the magnetic flux density does not comply with reference levels, the induced electric field has to be computed. The scalar potential finite difference (SPFD) implemented using the algebraic framework is used. In the low frequency range, displacement currents can be safely neglected [33], hence, the SPFD is given by:

$$\mathbf{G}^{\mathrm{T}}\mathbf{M}_{\sigma}\mathbf{G}\underline{\varphi} = -\mathrm{j}\omega\mathbf{G}^{\mathrm{T}}\mathbf{M}_{\sigma}\underline{\mathbf{a}}_{\mathrm{s}} \tag{2}$$

being $\underline{\varphi}$ the electric scalar potential and $\underline{\mathbf{a}}_{\mathrm{s}}$ the circulation of the magnetic vector potential (these variables are underlined because they are phasors, i.e. complex numbers). $\mathbf{G}$ is the edge-to-node incidence matrix representing the gradient topological operator and $\mathbf{M}_{\sigma}$ is the conductance matrix including the conductances computed considering all different biological tissues.

Equation (2) should be solved for each spectral line because the matrix $\mathbf{M}_{\sigma}$ depends on the frequency. However, in the low frequency range, the dependance is very weak and one can find an equivalent conductivity for each tissue suitable for the whole frequency range. This makes it possible to solve only one linear system with a normalized right hand side and

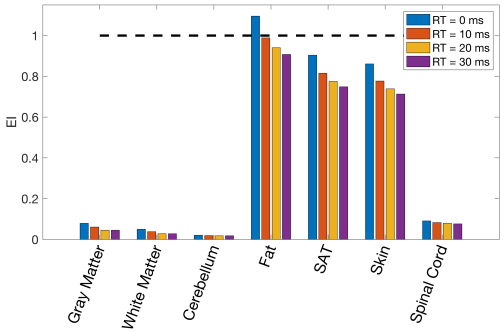

Fig. 17. Exposure index related to the induced electric field at some representative tissues. The highest exposure is registered at Fat tissue. The exposure becomes compliant for $RT > 10$ ms.

then to scale the result for each spectral line [33]. Finally, in agreement with the most recent literature on the subject, the metric used to extract the maximum electric field at each tissue is the 99.9th percentile [41].

The results of the evaluation are reported in Fig. 17 for some representative tissues. It is observed that for $RT = 0$ ms the exposure is not compliant because the induced electric field exceeds the basic restrictions in the fat tissue. However, thanks to the increase of the RT values, the exposure becomes compliant for $RT > 10$ ms. This confirms the effectiveness of the proposed mitigation action.

V. Conclusions

This paper has presented two practical actions aimed to the mitigation of the magnetic field generated by MFDC welding guns. Both actions are suggested by the principle of due diligence and aim to reduce as much as possible the exposure for the workers that operate in close proximity to the welding gun.

Investigating the first mitigation action, the paper points out that, the magnetic field created by the MF transformer can exceed the reference levels. The results of the paper show that a good reduction of the magnetic flux density can be obtained by using a shielding enclosure made of pure iron. This contributes to the reduction of the magnetic field levels in the pelvic area of the operators and reinforces the main hypothesis always used in the simulations: negligible contribution of the MF transformer. Measurements have been carried out in the region nearby the MF transformer in order to test different solutions. It is found that a shield made of pure iron should be preferred, especially with respect to pure conductive materials like aluminum. Moreover, it is observed that the MuMETAL, a material often used for shielding applications, is not effective in this context.

The second part of the work shows that another relevant reduction of the exposure can be obtained by increasing the rise time of the welding current pulse. It is shown that the increase of the rise time makes it possible to reduce the safety distance and the maximum value of the induced electric field in the human body. Considering a worst case scenario, a small increase of the rise time makes it possible a significant decrease of the exposure index, consequently, the compliance

can be met without changing anything else (current peak, distance between welding gun and operator, etc...).

Both the proposed solutions have the advantage that can be implemented easily without changing the architecture of the welding gun. In conclusion, the two presented mitigation actions are surely two ways to reduce the risk associated to the exposure to electromagnetic fields at workplaces where resistance spot welding is used.

REFERENCES

[1] Y. Cho and S. Rhee, "New technology for measuring dynamic resistance and estimating strength in resistance spot welding," *Measurement Science and Technology*, vol. 11, 2000.

[2] P. Podrzaj, I. Polajnar, J. Diaci, and Z. Kariz, "Expulsion detection system for resistance spot welding based on a neural network," *Measurement Science and Technology*, vol. 15, pp. 592–598, 2004.

[3] Y. Zhang, H. Wang, G. Chen, and X. Zhang, "Monitoring and intelligent control of electrode wear based on a measured electrode displacement curve in resistance spot welding," *Measurement Science and Technology*, vol. 18, pp. 867–876, 2007.

[4] L. Kuscer, I. Polajnar, and J. Diaci, "A method for measuring displacement and deformation of electrodes during resistance spot welding," *Measurement Science and Technology*, vol. 22, 2011.

[5] A. Simoncic and P. Podrzaj, "Image-based electrode tip displacement in resistance spot welding," *Measurement Science and Technology*, vol. 23, 2012.

[6] "C95.6 - IEEE Standard for Safety Levels with Respect to Human Exposure to Electromagnetic Fields, 0 - 3 kHz."

[7] "C95.1 - IEEE Standard for Safety Levels with Respect to Human Exposure to Radio Frequency Electromagnetic Fields, 3 kHz to 300 GHz."

[8] ICNIRP, "Guidelines for limiting exposure to time varying electric, magnetic and electromagnetic fields (up to 300 GHz)," *Health Phys*, vol. 74, no. 4, pp. 494–522, 1998.

[9] ICNIRP, "Guidance on determining compliance of exposure to pulsed and complex non-sinusoidal waveform below 100 kHz with ICNIRP guidelines," *Health Phys*, vol. 84, no. 3, pp. 383–387, 2003.

[10] ICNIRP, "Guidelines for limiting exposure to time-varying electric and magnetic fields (1 Hz to 100 kHz)," *Health Phys*, vol. 99, no. 6, pp. 818–836, 2010.

[11] L. Hasselgren and J. Luomi, "Geometrical aspects of magnetic shielding at extremely low frequencies," *IEEE Trans. Electromagn. Compat.*, vol. 37, no. 3, pp. 409–420, 1995.

[12] R. Olsen and P. Moreno, "Some observations about shielding extremely low-frequency magnetic fields by finite width shields," *IEEE Trans. Electromagn. Compat.*, vol. 38, no. 3, pp. 460–468, 1996.

[13] W. Frix and G. Karady, "A circuital approach to estimate the magnetic field reduction of nonferrous metal shields," *IEEE Trans. Electromagn. Compat.*, vol. 39, no. 1, pp. 24–32, 1997.

[14] "Mitigation techniques of power frequency magnetic fields originated from electric power systems," Tech. Rep. Worging group C4.204, International Council on Large Electric Systems (CIGRE'), 2009, ISBN: 978-2-85873-060-5.

[15] D. Bavastro, A. Canova, F. Freschi, L. Giaccone, and M. Manca, "Magnetic field mitigation at power frequency: design principles and case studies," *IEEE Trans. Ind. Appl.*, vol. 51, pp. 2009–2016, May 2014.

[16] A. Canova, F. Freschi, L. Giaccone, A. Guerrisi, and M. Repetto, "Magnetic field mitigation of power lines by means of passive loop: technical optimization," *COMPEL*, vol. 31, no. 3, pp. 870–880, 2012.

[17] L. Giaccone, D. Ragusa, and M. Khan, O. Manca, "Fast magnetic field modeling for shielding systems," *IEEE Trans. Magn.*, vol. 49, no. 7, 2013.

[18] F. Gustrau, A. Bahr, M. Rittweger, S. Goltz, and S. Eggert, "Simulation of induced current densities in the human body at industrial induction heating frequencies," *IEEE Trans. Electromagn. Compat.*, vol. 41, no. 4, pp. 480–486, 1999.

[19] R. Doebbelin, T. Winkler, and A. Lindemann, "Environmental emc aspects of resistance welding equipment," *Electrical Power Quality and Utilisation, Journal*, vol. 11, no. 2, pp. 41–48, 2005.

[20] D. Desideri and A. Maschio, "Magnetic field emissions up to 400 kHz from a welding equipment," in *Proc. Int. Symp. Electromagnetic Compatibility*, pp. 151–156, Barcelona, 2006.

[21] M. Gonzalez, A. Peratta, and D. Poljak, "Boundary element modeling of the realistic human body exposed to extremely-low-frequency (elf) electric fields: Computational and geometrical aspects," *IEEE Trans. Electromagn. Compat.*, vol. 49, no. 1, pp. 153–162, 2007.

[22] X. L. Chen, A. Umenei, D. Baarman, N. Chavannes, V. De Santis, J. Mosig, and N. Kuster, "Human exposure to close-range resonant wireless power transfer systems as a function of design parameters," *IEEE Trans. Electromagn. Compat.*, vol. 56, no. 5, pp. 1027–1034, 2014.

[23] V. Cirimele, F. Freschi, L. Giaccone, L. Pichon, and M. Repetto, "Human exposure assessment in dynamic inductive power transfer for automotive applications," *IEEE Trans. Magn.*, vol. 53, n. 3, art. n. 5000304, June 2017.

[24] "Directive of the european parliament and of the council of 29 april 2004 On the Minimum Health and Safety Requirements Regarding the Exposure of Workers to the Risks Arising From Physical Agents (Electromagnetic Fields) European Parliament and Council."

[25] "Directive 2013/35/EU of the European Parliament and of the Council of 26 June 2013 on the minimum health and safety requirements regarding the exposure of workers to the risks arising from physical agents (electromagnetic fields) (20th individual Directive within the meaning of article 16(1) of directive 89/391/EEC) and repealing directive 2004/40/EC."

[26] H. Heinrich, "Assessment of non-sinusoidal, pulsed or intermittent exposure to low frequency electric and magnetic fields," *Health Phys*, vol. 96, no. 6, pp. 541–546, 2007.

[27] V. De Santis, X. L. Chen, I. Laakso, and A. Hirata, "On the issues related to compliance of LF pulsed exposures with safety standards and guidelines," *Phisycs in Medicine and Biology*, vol. 58, pp. 8597–8607, 2013.

[28] K. Jokela, "Restricting exposure to pulsed and broadband magnetic fields," *Health Phys*, vol. 79, no. 4, pp. 373–388, 2000.

[29] A. Canova, F. Freschi, and M. Repetto, "Evaluation of workers exposure to magnetic fields," *The European Physical Journal Applied Physics*, vol. 52, no. 2, 2010.

[30] A. Canova, F. Freschi, L. Giaccone, and M. Repetto, "Exposure of working population to pulsed magnetic fields," *IEEE Trans. Magn.*, vol. 46, no. 8, pp. 2819–2822, 2010.

[31] F. Dughiero, M. Forzan, and E. Sieni, "A numerical evaluation on Electromagnetic fields exposure on real human body models until 100 kHz," *COMPEL*, vol. 29, pp. 1552–1561, 2010.

[32] R. Doebbelin, T. Winkler, and A. Lindemann, "Influence of the design of resistance welding equipment on the evaluation of magnetic field exposure of operators," in *PIERS Proceedings*, pp. 1400–14005, Marrakesh, Marocco, March 20-23, 2011 2005.

[33] A. Canova, F. Freschi, L. Giaccone, and M. Manca, "A Simplified Procedure for the Exposure to the Magnetic Field Produced by Resistance Spot Welding Guns," *IEEE Trans. Magn.*, in press.

[34] "EN 50505 - Basic standard for the evaluation of human exposure to electromagnetic fields from equipment for resistance welding and allied processes."

[35] "EN 50444 - Basic standard for the evaluation of human exposure to electromagnetic fields from equipment for arc welding and allied processes."

[36] D. Bavastro, A. Canova, L. Giaccone, and M. Manca, "Numerical and experimental development of multilayer magnetic shields," *Electric Power Systems Research*, vol. 116, pp. 374–380, 2014.

[37] L. Giaccone, D. Giordano, and G. Crotti, "Identification and Correction of Artifact in the Measurement of Pulsed Magnetic Fields," *IEEE Trans. Instrum. Meas.*, vol. 66, pp. 1260–1266, June 2017.

[38] A. Canova, F. Freschi, and L. Giaccone, "How safe are spot welding guns to use?," *IEEE Ind. Appl. Mag.*, vol. 24, pp. pp 39–47, May-June 2018.

[39] T. Dawson, K. Caputa, and M. Stuchly, "Electric fields induced in humans and rodents by 60 Hz magnetic fields," *Physics in Medicine and Biology*, vol. 47, pp. 2561–2568, 2002.

[40] A. Christ, W. Kainz, E. Hahn, K. Honegger, M. Zefferer, E. Neufeld, W. Rascher, R. Janka, W. Bautz, J. Chen, B. Kiefer, P. Schmitt, H. Hollenbach, J. Shen, M. Oberle, D. Szczerba, A. Kam, G. J.W., and N. Kuster, "The virtual family – development of surface-based anatomical models of two adults and two children for dosimetric simulations," *Physics in Medicine and Biology*, vol. 55, no. 2, pp. 23–38, 2010.

[41] J. Gomez-Tames, I. Laakso, Y. Haba, A. Hirata, D. Poljak, and K. Yamazaki, "Computational artifacts of the in situ electric field in anatomical models exposed to low-frequency magnetic field," *IEEE Trans. Electromagn. Compat.*, vol. 60, pp. pp 589–597, June 2018.

Luca Giaccone (M'14-SM'15) was born in Cuneo, Italy, in 1980. He received the Laurea degree and the Ph.D. degree in Electrical Engineering from the Politecnico di Torino, Turin, Italy, in 2005 and 2010, respectively. Prof. Giaccone worked on several areas of the electrical engineering: optimization and modeling of complex energy systems, computation of electromagnetic and thermal fields, energy scavenging, magnetic field mitigation, EMF dosimetry, compliance of LF pulsed magnetic field sources. Since 2017 he is associate professor with the Politecnico di Torino, Dipartimento Energia. He is member of the IEEE since 2014 and he has been elevated to senior member in February 2015. Since November 2015 he is member of the IEEE International Committee on Electromagnetic Safety - Technical Committee 95 - Subcommittee 6 that works in the field of EMF Dosimetry Modeling. Since September 2017, he is also member of the national committee CEI-106 dealing with human exposure to electromagnetic fields.

Vincenzo Cirimele (M'15) was born in Belvedere Marittimo, Italy, in 1987. In 2013, he received the M.Sc. degree in Electrical Engineering (summa cum laude) from the Politecnico di Torino, Turin, Italy, where he is presently enrolled as Research Fellow at the Department of Energy. He received the Ph.D. in Electronics Engineering from the Politecnico di Torino and the PhD in Electrical Engineering form the Université Paris-Sacaly, France in 2017. From 2015 to 2016 he joined the CNRS laboratory Génie électrique et électronique de Paris (GeePs) in France. His main research interests include protection of people from the magnetic field at industrial frequency, electromagnetic modeling and optimization of special electrical and electromechanical devices, inductive power transmission for electric vehicles. Since July 2018 he is member of the national IEC Technical Committee 14 - Power Transformers.

Aldo Canova (SM'15) a was born in Biella, Italy, in 1967. He received the Laurea and Ph.D. degrees in electrical engineering from the Politecnico di Torino, Turin, Italy, in 1992 and 1996, respectively. Since October 1995, he has been a Researcher and in 2003, he became an Associate Professor with the Dipartimento di Ingegneria Elettrica, Politecnico di Torino. He is involved in research activities related to the numerical computation of electromagnetic fields in the area of power devices. He is the author of about 180 scientific publications in international conference proceedings and international journals and an inventor in seven patents. Prof. Canova is a member of the Comitato Elettrotecnico Nazionale (CEI) serving on Technical Committee CT106 (Methods for the assessment of electric, magnetic and electromagnetic fields associated with human exposure) since 2004. He was a member of the International Council on Large Electric Systems (CIGRE) in Working Group 36.04 on Magnetic field mitigation techniques during 2002-2005.